CORRIGENDUM

DOI: 10.3892/ijo.2023.5528

Role of the EZH2/miR-200 axis in STAT3-mediated OSCC invasion

YU WANG, WENYU GUO, ZHAOQING LI, YANSHENG WU, CHAO JING, YU REN, MINGHUI ZHAO, LINGPING KONG, CHAO ZHANG, JIABIN DONG, YU SHUANG, SHANSHAN SUN, JINLIANG CHEN, CHUANQIANG WU, YU QIAO, XIN QU, XUDONG WANG, LUN ZHANG, RUI JIN and XUAN ZHOU

Int J Oncol 52: 1149-1164, 2018; DOI: 10.3892/ijo.2018.4293

Following the publication of the above article, an interested reader drew to the authors' attention that, in Figs. 7A and 8A. apparently the same mouse had been featured to represent two different experimental groups, albeit displaying distinct fluorescence values. Moreover, following an independent investigation in the Editorial Office, an additional instance of probable data duplication was also noted, comparing between the 'SCC15 / si-NC' cell migration image in Fig. 2D and the 'SCC15-EV' migration assay image in Fig. 1C.

After having consulted their original data, the authors realized that these errors arose during the process of assembling the images for Figs. 2 and 8. First, the image for the DZNep (42d) experiment in Fig. 7A had inadvertently been used for the mimic NC (7d) experiment in Fig. 8A; moreover, the 'SCC15 / si-NC' cell migration image in Fig. 2D had been selected incorrectly.

The revised versions of Figs. 2 and 8, showing the correct data for the the 'SCC15 / si-NC' cell migration image in Fig. 2D and the mimic NC (7d) experiment in Fig. 8A, are shown on the next two pages. The authors regret that these errors went unnoticed prior to publication, and thank the Editor of *International Journal of Oncology* for allowing them the opportunity to publish this corrigendum. All the authors agree with the publication of this corrigendum; furthermore, they also apologize to the readership of the journal for any inconvenience caused.

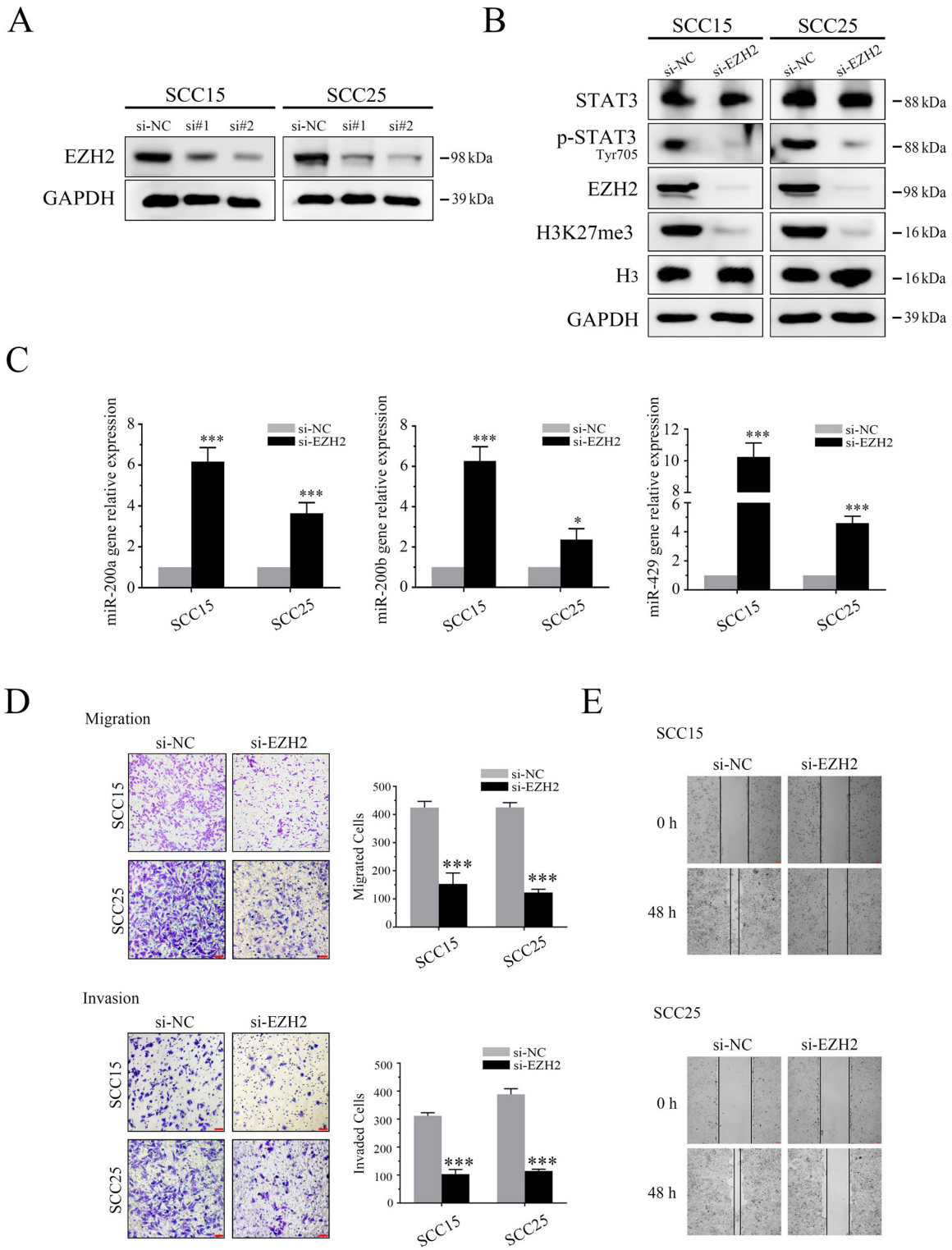

Figure 2. EZH2/miR-200/b/a/429 axis regulates the invasiveness of OSCC cells *in vitro*. (A) Following transfection with EZH2 siRNAs (si#1 and si#2) for 3 days, the expression levels of EZH2 were detected using western blotting. (B) OSCC cells underwent western blot analysis using antibodies specific to STAT3, p-STAT3 (Tyr705), EZH2, H3K27me3, H3 and GAPDH. EZH2 siRNA markedly inhibited EZH2 and H3K27me3 expression. In addition, p-STAT3 (Tyr705), but not STAT3, was suppressed by EZH2 depletion. (C) EZH2 siRNA induced miR-200b/a/429 expression. (D) Results of a Transwell assay demonstrated that EZH2 knockdown markedly attenuated migration (without Matrigel) and invasion (with Matrigel) of SCC25 and SCC15 cells (scale bar, 100 µm; magnification, ×40). (E) Scratch assay demonstrated that EZH2 silencing markedly delayed wound healing in SCC25 and SCC15 cells (magnification, ×40). *P<0.05 and ***P<0.001 vs. si-NC group. EZH2, enhancer of zeste homolog 3; H3, histone 3; H3K27me3, trimethylation of lysine 27 in H3; miR-200b/a/429, microRNA-200b, -200a and -429; NC, negative control; OSCC, oral squamous cell carcinoma; p-STAT3, phosphorylated-STAT3; siRNA/si, small interfering RNA; STAT3, signal transducer and activator of transcription 3.

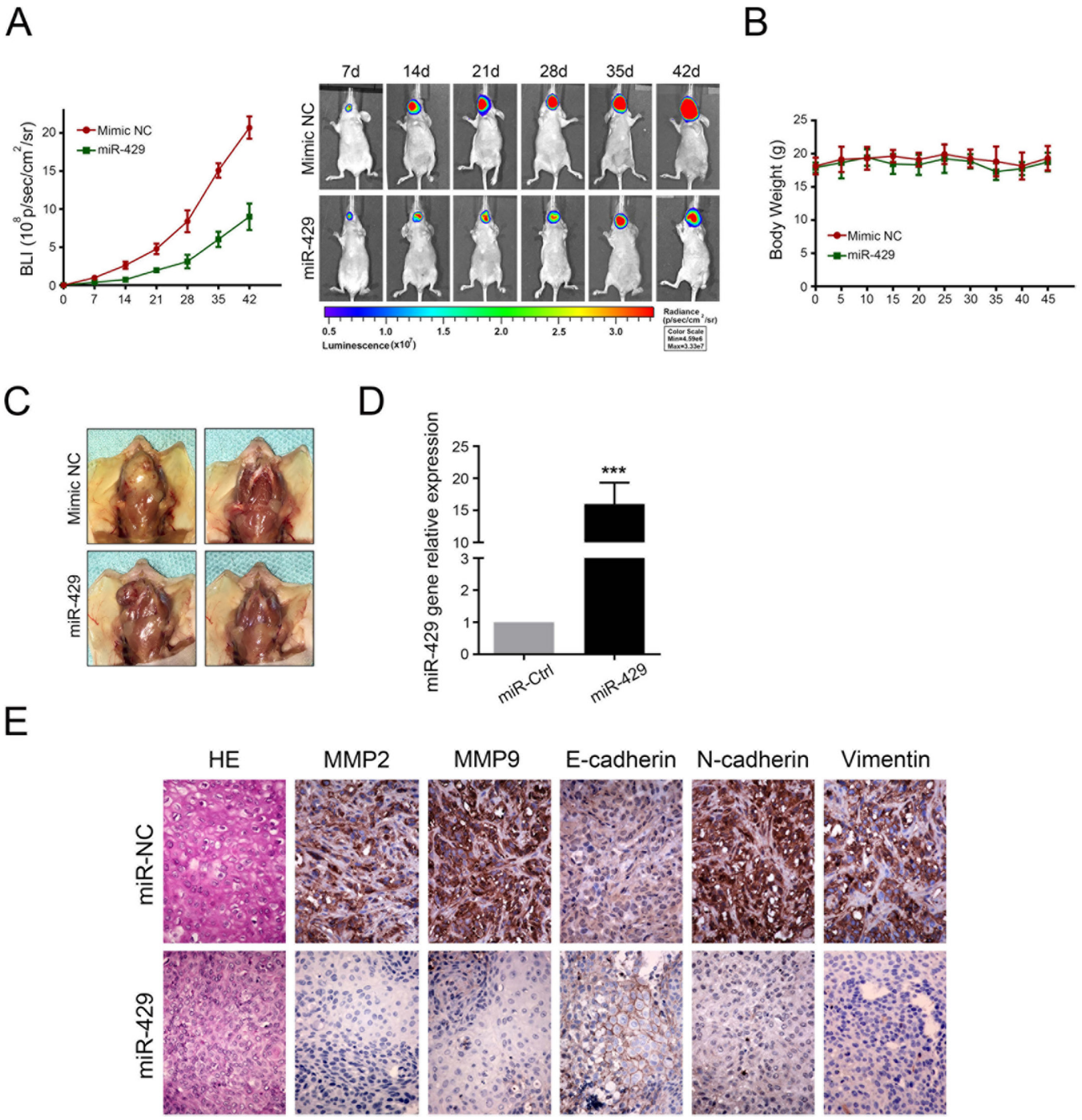

Figure 8. miR-429 inhibits tumor progression in the orthotopic mouse model of OSCC. (A) Representative bioluminescence images of mice implanted with orthotopic tumors and treated intraperitoneally with miR-Ctrl (10 nM/mice) or miR-429 (10 nM/mice) every 3 days. (B) Quantification of body weight in control and miR-429-treated mice. (C) miR-429 inhibits OSCC local invasion in an orthotopic mouse model. (D) Tumor diameter and volume were measured. (E) Quantitative polymerase chain reaction was used to detect the expression levels of mir-429 in OSCC tumor sections. (F) Tumor samples from control and miR-429-treated mice underwent immunohistochemistry for MMP2, MMP9, E-cadherin, N-cadherin and Vimentin (scale bar, 100 µm; magnification, ×200). ***P<0.001 vs. miR-Ctrl group. Ctrl, control; H&E, hematoxylin and eosin; miR, microRNA; MMP, matrix metalloproteinase; NC, negative control.